On the Optimization of Damping Enhancement in a Power System with a Hybrid HVDC Link

Chamorro, Harold; Torkzadeh, Roozbeh; Kotb, Omar; Rouzbehi, Kumars; Escaño, Juan Manuel; Gonzalez-Longatt, Francisco; Bellmunt, Oriol Gomis; Toma, Lucian; Sood, Vijay K

Accepted version of article in
2019 IEEE PES Innovative Smart Grid Technologies Europe (ISGT-Europe)

Original version:
DOI: 10.1109/ISGTEurope.2019.8905612

On the Optimization of Damping Enhancement in a Power System with a Hybrid HVDC Link

Harold R. Chamorro, *Senior Member, IEEE,* Roozbeh Torkzadeh, *Member, IEEE,* Omar Kotb, *Member, IEEE,* Kumars Rouzbehi, *Senior Member, IEEE,* Juan Manuel Escaño, *Senior Member, IEEE,* Francisco Gonzalez-Longatt, *Senior Member, IEEE,* Oriol Gomis Bellmunt, *Senior Member, IEEE,* Lucian Toma, *Senior Member, IEEE,* and Vijay K. Sood, *Fellow Member, IEEE,*

***Abstract*—Hybrid HVDC links incorporate both Line Commutated Converters (LCC) and Voltage Source Converters (VSC) systems, thereby gathering the benefits of both technologies. Supplementary Power Oscillation Damping (POD) controllers can be added to both LCCs and VSCs to help enhance the power system stability against disturbances, such as short circuits. However POD controller tuning can be a delicate process, due to the highly non-linear and complex nature of the involved power system, which might induce adverse interactions leading to a reduced damping. This paper proposes the application of the Simulated Annealing Algorithm (SAA) for tuning the POD controllers parameters, with the purpose of optimizing the performance of POD controllers in the power system. The damping performance is evaluated in case of multiple disturbances in a test power system. The results show the ability of the proposed technique to enhance the performance of the POD controllers under various operating conditions.**

***Index Terms*—Hybrid HVDC, LCC, Power Oscillation Damping, Simulated Annealing Algorithm, VSC.**

I. Introduction

FUTURE DC grids are envisioned to incorporate hybrid (High Voltage Direct Current) HVDC transmssion as a potential solution for interconnecting multiple point-to-point HVDC links for the purpose of forming an overlay grid. DC grids are expected to provide a future solution for large-scale integration of renewable energy sources [1]- [2], with the DC grid spanning multiple transmission systems across national borders. The maturity of the HVDC technology enables to provide active and reactive power control independently [3], besides contributing to the transfer capacity [4], [5]. The use of hybrid HVDC combining both LCC and VSC technologies brings the advantages of both systems such the ability to connect to weak and strong grids, as well as the reduced cost of the grid. [6], [7].

Countries like China and India have ambitious electrical infrastructure projections that are currently facing several operational challenges to expand their power systems by building new AC transmission lines. By merging HVDC links, the possibility of transferring power from remote areas is expected to be improved [8], [9]. Multiple plans are also being considered for transmission system expansion in through HVDC interconnections in Europe, especially in the NORDEL and the Union for the Coordination of the Transmission of Electricity (UCTE). Those plans involve connections between Norway, Sweden, Denmark, the Netherlands and Germany in order to improve the non-synchronous generation, and release the bottlenecks congestion [10].

Power Oscillation Damping (POD) controllers are a class of supplementary controllers used in conjunction with converter controls for the purpose of enhancing the stability of the AC power system. POD control contributes to the damping of local-area and inter-area oscillations, thereby boosting the transfer capability and improving the system transient stability under large disturbances [11]. Additionally, POD supplementary controllers enable Transmission System Operators (TSO) improve network capacity. However, although the POD control loop involved can be a simple one, its tuning requires a vast designer's expertise and/or simulating several tests and scenarios when finding the proper gain values. Additionally, the system non-linearity presents a challenge to the selection of a specific nominal operating point. Thus, the differing operating conditions might require the change of POD controllers tuning as well.

The residue method has traditionally been used to tune the POD controller parameters [11]. However, the controller settings obtained are dependent on the operating point of the system, and thus, an optimal tuning across multiple operating conditions is not guaranteed [12].

On the other hand, stochastic and combinatorial optimization techniques have been applied to tuning controllers in power systems applications [13], [14], and are characterized by flexibility in adapting to the changing operating points of the system. For instance, Genetic Algorithms (GA) have been applied for optimizing the Flexible AC Transmission Systems (FACTs) controllers with the objective of minimizing the undesired low-frequency oscillations [15]. In [16], Bee coloniy

Harold R. Chamorro is with KTH, Royal Institute of Technology, Stockholm, Sweden (hr.chamo@ieee .org).

Roozbeh Torkzadeh is with Eindhoven University of Technology, 5600 MB Eindhoven, The Netherlands (rtorkzadeh@ieee .org & r.torkzadeh@tue .nl).

Omar Kotb is with MathWorks AB, Stockholm, Sweden (omarkotb@mathworks .com).

Kumar Rouzbehi and Juan Manuel Escaño are with Seville University, Seville, Spain (krouzbehi@us .es & jescano@us .es).

Francisco Gonzalez-Longatt is with University of South-Eastern Norway, Porsgrunn, Norway. (f.gonzalez-longatt@usn .no)

Oriol Gomis-Bellmunt is with CITCEA-UPC, Departament dEnginyeria Electrica, Universitat Politecnica de Catalunya, Barcelona, Spain.

Lucian Toma is with University Politehnica of Bucharest, Bucharest, Romania.(lucian.toma@ieee .org & lucian.toma@upb .ro).

Vijay K. Sood is with the Department of Electrical and Computer Engineering of the University of Ontario, Institute of Technology, Ontario, Canada (vijay.sood@uoit .ca)

optimization method has been used for the same purpose and it is been tested in a large power system. Simulated Annealing Algorithm (SAA) has proved to be an efficient optimization algorithm for finding global control parameters [17]. For instance in [18], SAA has been applied to an Interline Power Flow Controller (IPFC) POD for damping low frequency oscillations and it is tested in the two-areas test power system for validating the results.

This paper proposes the application of SAA for optimizing the POD controllers' performance in a power system with a hybrid HVDC link. The application of SAA is done with the purpose of adjusting the controller parameters to suit changing system conditions. Time-domain simulations are used to test the controllers' performance in a test power system.

The paper is organized as follows: Section II describes the system modeling and the POD controller configuration. Section III presents the proposed POD function for the hybrid HVDC link and optimization problem. The test system is described in Section IV. The simulation results and discussions are presented in Section V, and finally Section VI presents the conclusion and future works.

II. AC/DC Power System Modeling

A. LCC model

The LCC represented by a response model and shown in Fig. 1. The state equation for DC current I_{dc} is given by:

$$\dot{I}_{dc} = \frac{1}{L_{dc}}(V_{LCC} - V_{dc1}) \tag{1}$$

where L_{dc} is the smoothing reactor, V_{LCC} is the DC voltage at the LCC, and V_{dc1} is the DC voltage at the DC line terminal.

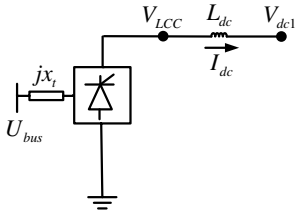

Fig. 1. LCC model connected to the DC line.

B. VSC model

The VSC is represented by an average model, and shown in Fig. 2. The VSC's controlled voltage is given by:

$$\bar{E}_c = E_c\big(cos(\gamma_c) + jsin(\gamma_c)\big) = E_d + jE_q \tag{2}$$

where E_d and E_q are the controlled voltage components of the VSC, V_i is the DC voltage at the VSC terminal, C_{dc} is the equivalent capacitance across the DC side of the VSC, x_T is the reactance of converter transformer, $\bar{U}$ is the AC voltage of the converter bus, and $\bar{E}_c$ is the controllable voltage of the VSC. The VSC's voltage magnitude and phase angle are defined as:

$$E_c = \sqrt{E_d^2 + E_q^2} \tag{3}$$

$$\gamma_c = tan^{-1}(\frac{E_q}{E_d}) \tag{4}$$

Neglecting the power losses in the converter, the active and reactive power exchanged between the VSC and AC system are given as:

$$P_c = \frac{UE_c}{x_T}sin(\theta - \gamma_c) = \frac{U}{x_T}(E_d sin\theta - E_q cos\theta) \tag{5}$$

$$Q_c = \frac{U^2}{x_T} - \frac{UE_c}{x_T}cos(\theta - \gamma_c) = \frac{U^2}{x_T} - \frac{U}{x_T}(E_d cos\theta + E_q sin\theta) \tag{6}$$

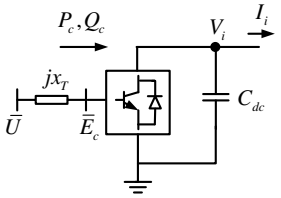

Fig. 2. VSC model connected to the DC line.

C. DC Line Model

The DC line model is shown in Fig. 3. The state equation of DC line current is given as:

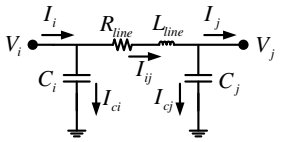

Fig. 3. DC line model.

D. LCC and VSC controller models

The LCC firing angle α is used to regulate the DC current, as shown in Fig. 4. The equation for the LCC firing angle is given by:

$$\alpha = x_\alpha + k_p^{LCC}(I_{dc} - I_{dcref}) + u_{POD1} \tag{7}$$

where k_p^{LCC} is the proportional gain, x_{alpha} is the controller's state variable, and I_{dcref} is the DC current set-point value. The POD controller's contribution is given by u_{POD1}. The controller's state equation is given by:

$$\dot{x}_\alpha = k_i^{LCC}(I_{dc} - I_{dcref}) \tag{8}$$

On the other hand, based on the selected control modes at the VSC, the controllable voltage component E_d can be regulated to control either the AC voltage generated by the VSC, or the reactive power exchanged with the connected AC system. Similarly, the component E_q can be regulated to

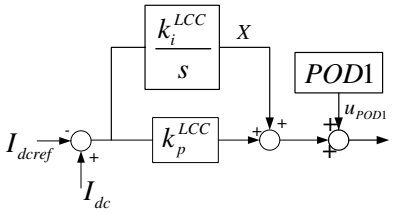

Fig. 4. DC current control at the LCC.

control either the DC voltage, or the active power exchanged with the connected AC system. The controllers for E_d and E_q are shown in Fig. 5 and Fig. 6, respectively. The contribution from auxiliary POD controllers is also shown in the figures. In case of disturbances, the POD controller contributes to improve the damping in the connected AC system. In case of reactive power control, the controller equations in Fig. 5 are given by:

$$\begin{aligned} E_d &= k_p^{E_d}(Q_{cref} - Q_c) + x_{E_d} + u_{POD} \\ \dot{x}_{E_d} &= k_i^{E_d}(Q_{cref} - Q_c) \end{aligned} \tag{9}$$

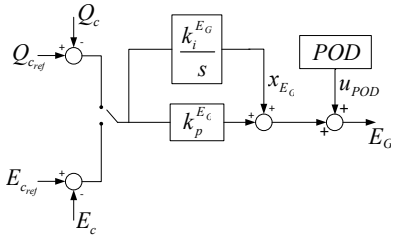

Fig. 5. AC voltage/reactive power control at the VSC.

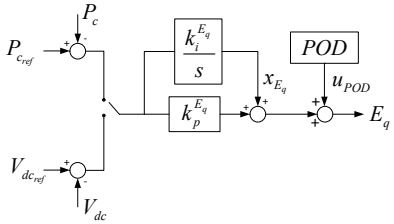

Fig. 6. DC voltage/active power control at the VSC.

In case of DC voltage control, the controller equations in Fig. 6 are given by:

$$E_q = k_p^{E_q}(V_{dcref} - V_{dc}) + x_{E_q} + u_{POD} \tag{10}$$

$$\dot{x}_{E_q} = k_i^{E_q}(V_{dcref} - V_{dc}) \tag{11}$$

On the other hand, in case of active power control through E_q, the controller equations are given by:

$$E_q = k_p^{E_q}(P_{cref} - P_c) + x_{E_q} + u_{POD} \tag{12}$$

$$\dot{x}_{E_q} = k_i^{E_q}(P_{cref} - P_c) \tag{13}$$

E. Generator model

The generators are represented by one-axis model together with Automatic Voltage Regulator (AVR) and Power System Stabilizer (PSS). The state equations of the generators are given as:

$$\begin{aligned} \dot{\delta}_i &= \omega_i \\ \dot{\omega}_i &= \tfrac{1}{M_i}(P_{mi} - \tfrac{U_i E_{qi}^{'} sin(\delta_i - \theta_i)}{x_{di}^{'}}) \end{aligned} \tag{14}$$

$$\dot{E}^{'}{}_{qi} = \frac{1}{T_{di}^{'}}(E_{fdi} - \frac{x_{di}}{x_d^{'}}E_{qi}^{'} + \frac{x_{di} - x_{di}^{'}}{x_{di}^{'}}U_i cos(\delta_i - \theta_i)) \tag{15}$$

$$\begin{aligned} \dot{E}_{fdi} =& \frac{1}{T_{ei}}(-E_{fdi} + K_{Ai}U_{refi} - K_{Ai}U_i) + \\ & \frac{T_{1i}T_{3i}}{T_{2i}T_{4i}}K_{PSSi}\omega_i - \frac{T_{1i}T_{3i}}{T_{2i}T_{4i}}S_{1i} + \frac{T_{3i}}{T_{4i}}S_{2i} + S_{3i} \end{aligned} \tag{16}$$

$$\dot{S}_{1i} = \frac{K_{PSSi}}{T_{wi}}\omega_i - \frac{1}{T_{wi}}S_{1i} \tag{17}$$

$$\begin{aligned} \dot{S}_{2i} =& \frac{K_{PSSi}(T_{2i} - T_{1i})}{T_{2i}^2}S_{1i}\omega_i - \\ & \frac{T_{2i} - T_{1i}}{T_{2i}^2}S_{1i} - \frac{1}{T_{2i}}S_{2i} \end{aligned} \tag{18}$$

$$\begin{aligned} \dot{S}_{3i} =& K_{PSSi}\frac{T_{1i}}{T_{2i}}\frac{T_{4i} - T_{3i}}{T_{4i}^2}\omega_i - \frac{T_{1i}}{T_{2i}}\frac{T_{4i} - T_{3i}}{T_{4i}^2}S_{1i} + \\ & \frac{T_{4i} - T_{3i}}{T_{4i}^2}S_{2i} - \frac{1}{T_{4i}}S_{3i} \end{aligned} \tag{19}$$

where $i = 1, 2, ..., n_g$, δ_i is the generator rotor angle, ω_i is the generator speed, M_i is the generator constant, P_{mi} is the input mechanical power to the generator, U_i is the generator bus voltage, θ_i is the generator bus angle, $E_{qi}^{'}$ is the internal emf of the generator, E_{fdi} is the exciter voltage, x_d and $x_d^{'}$ are the equivalents of transformer reactance in addition to generator's transient and steady state reactances, respectively, K_{Ai} is the exciter gain of the AVR, and U_{refi} is the reference voltage of the AVR. S_{1i}, S_{2i}, and S_{3i} are the PSS states, K_{PSSi} is the PSS gain, T_{1i}, T_{2i}, T_{3i}, and T_{4i} are the lead-lag constants of the PSS, and T_{wi} is the washout filter constant of the PSS.

III. Simulated Annealing Algorithm Application

Simulated annealing algorithm (SAA) is a stochastic global optimization algorithm, which is able to jump out from local minimum to achieve the global minimum [19]. The SAA is divided into six major components including

1) cost function,
2) initial condition,
3) move generation
4) probability function
5) cooling schedule
6) stopping condition.

Given an cost function, an initial solution (condition) is generated. Then, in each step, the move generation function will control the perturbation around the current solution. The probability function that is affected by the temperature identifies the acceptance of a new status. Next, the temperature is

cooled down to archive a more contingent acceptance criterion for the same probability function, therefore, a worse state is harder to be accepted in the future. Finally, during the SAA procedures, the cost function value eventually converges, and the search is terminated if the stopping condition is satisfied. In this paper, the SAA is used to find the optimal value of the tunable k_{POD} to minimize the power oscillations.

A. Used SAA Pseudo code

Algorithm 1 Simulated Annealing Algorithm (SAA) Pseudo code

1: **Select** an initial state $i \in S$;
2: **Select** an initial temperature $T > 0$;
3: **Set** temperature change counter $t = 0$;
4: *Repeat*
5: **Set** repetition counter $n = 0$;
Repeat **Generate** state j, a neighbour of i; **Calculate** $\delta = f(j) - f(i)$; *If* $\delta < 0$ then $i := j$ *else if* $random(0,1) < exp(-8/T)$ then $i := j$;
$n := n + l$;
until $n = N(t)$;
6: $t := t + l$;
7: $T := T(t)$;
8: *Until* stopping criterion true.
9: **Return** T

B. Cost Function

The formulation of optimization problem is mentioned in (20). In addition, for defining the lower and upper boundaries for the k, it is considered that $k \in [-100, 100]$. Furthermore, the initial condition is assumed as $k_{POD} = -20$.

$$\begin{aligned} &Given: \hat{x} = k; \\ &Minimize: f(\hat{x}) = \frac{1}{n_{sample}} \sum_{i=1}^{n_{sample}} (P_i - \bar{P})^2 \\ &ST: -100 \leq k \leq 100 \end{aligned} \tag{20}$$

where, P_i is the value for active power of *DC line* in i-th step of simulation, $\bar{P}$ is the average of P_i and n_{sample} is total number of simulation steps.

IV. Test Case System

The test system is shown in Fig. 7. It comprises an AC system in parallel with a DC system. The AC/DC power system model is described by a set of Differential Algebraic Equations (DAEs) summarized as:

$$\dot{x} = f(x, y, \eta) \tag{21}$$
$$0 = g(x, y, \eta) \tag{22}$$

where x is the vector of state equation described in Sections II and II-D, y is the vector of algebraic variables as formulated by load flow solution [11], and η is the vector of system parameters, while f and g are the differential and algebraic functions describing the system, respectively.

As the DC line connecting the LCC and VSC was considered short, the shunt capacitance of the line was neglected, hence the line was dynamically represented only by its series resistance (R_{dc}) and inductance (L_{dc}).

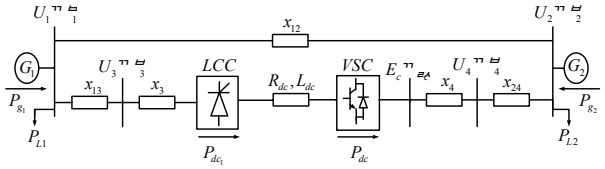

Fig. 7. Test power system with hybrid HVDC link.

V. Simulation Results

In this paper, the optimal value of k_{Damp} is found for different operation scenarios. Then, by using all the optimal values for k_{Damp}, a look-up table is formed. This look-up table is used to tune the POD function regarding the transferring power for different operational scenarios.

Simulation results for different operational scenarios with the optimal k_{Damp} value for transferring power of 0.3 p.u., 0.4 p.u., and 0.5 p.u. are depicted in Figs. 8, 9 and 10, respectively.

As it is clearly shown in Fig. 8, the proposed optimal POD function is capable to damp the oscillations, just a few second after the starting of oscillation.
However, by comparing Fig 8 and 10, it is obvious that by decreasing the flow of power through the link, it takes longer time for the optimal POD function to damp the oscillations. Nonetheless, the proposed POD can damp the oscillations in all different operational conditions.

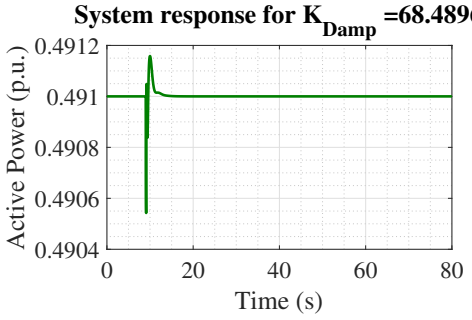

Fig. 8. Optimal POD for $P_{transfer} = 0.5 p.u.$

A second scenario is including by activating the supplementary control in the VSC station. The results for transfering power of 0.3 p.u., and 0.4 p.u. are depicted in Figs. 11, and 12, respectively.

VI. Conclusion

This paper presents the application of SAA to tune the POD controllers in a hybrid HVDC system. The SAA is a heuristic optimization method that is capable of dealing with complex dynamical systems with high nonlinearity. The combined AC/DC power system was described by a DAE model, with the

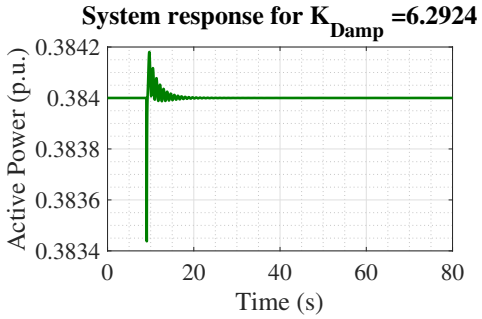

Fig. 9. Optimal POD for $P_{transfer} = 0.4p.u.$

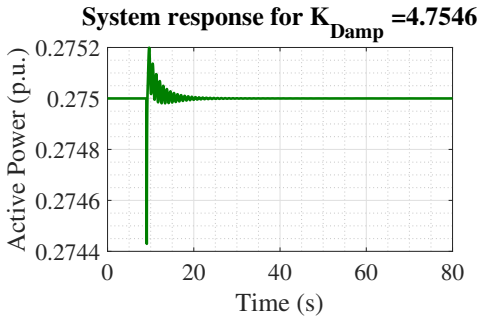

Fig. 10. Optimal POD for $P_{transfer} = 0.3p.u.$

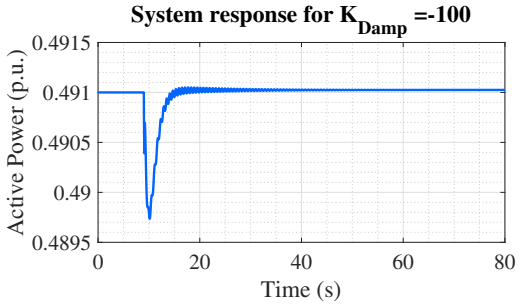

Fig. 11. Optimal POD for $P_{transfer} = 0.3p.u.$

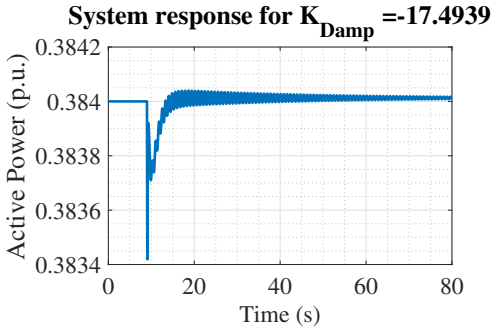

Fig. 12. Optimal POD for $P_{transfer} = 0.4p.u.$

differential equations describing the dynamic elements of the system, such as generators and converters, while the algebraic equations representing the power flow problem formulation. The results show the ability of the proposed algorithm to fine tune the controller parameters to minimize the power oscillations that take place following various disturbances in the system, as shown via time-domain simulations.

REFERENCES

[1] C. A. Ordonez, A. Puentes, H. R. Chamorro, and G. Ramos, "p - q theory for active compensation applied to supergrids and microgrids," in *2012 Workshop on Engineering Applications*, pp. 1–6, May 2012.

[2] A. Heidary, H. Radmanesh, K. Rouzbehi, and J. Pou, "A dc-reactor based solid-state fault current limiter for hvdc applications," *IEEE Transactions on Power Delivery*, pp. 1–1, 2019.

[3] H. R. Chamorro, N. L. Diaz, J. J. Soriano, and H. E. Espitia, "Active and reactive power flow fuzzy controller for vsc hvdc using dbr and dbr type 2," in *2011 Annual Meeting of the North American Fuzzy Information Processing Society*, pp. 1–6, March 2011.

[4] W. Litzenberger, K. Mitsch, and M. Bhuiyan, "When it's time to upgrade: Hvdc and facts renovation in the western power system," *IEEE Power and Energy Magazine*, vol. 14, pp. 32–41, March 2016.

[5] O. Kotb, M. Ghandhari, R. Eriksson, R. Leelaruji, and V. K. Sood, "Stability enhancement of an interconnected ac/dc power system through vsc-mtdc operating point adjustment," *Electric Power Systems Research*, vol. 151, pp. 308 – 318, 2017.

[6] O. Kotb, M. Ghandhari, R. Eriksson, and V. K. Sood, "On small signal stability of an ac/dc power system with a hybrid mtdc network," *Electric Power Systems Research*, vol. 136, pp. 79 – 88, 2016.

[7] I. M. Sanz, P. D. Judge, C. E. Spallarossa, B. Chaudhuri, T. C. Green, and G. Strbac, "Effective damping support through vsc-hvdc links with short-term overload capability," in *2017 IEEE PES Innovative Smart Grid Technologies Conference Europe (ISGT-Europe)*, pp. 1–6, Sep. 2017.

[8] H. Zhou, Y. Su, Y. Chen, Q. Ma, and W. Mo, "The china southern power grid: Solutions to operation risks and planning challenges," *IEEE Power and Energy Magazine*, vol. 14, pp. 72–78, July 2016.

[9] G. D. Kamalapur, V. R. Sheelavant, S. Hyderabad, A. Pujar, S. Baksi, and A. Patil, "Hvdc transmission in india," *IEEE Potentials*, vol. 33, pp. 22–27, Jan 2014.

[10] B. M. Buchholz, D. Povh, and D. Retzmann, "Stability analysis for large power system interconnections in europe," in *2005 IEEE Russia Power Tech*, pp. 1–7, June 2005.

[11] O. Kotb, M. Ghandhari, R. Eriksson, and V. K. Sood, "Control of a hybrid hvdc link to increase inter-regional power transfer," in *2016 18th Mediterranean Electrotechnical Conference (MELECON)*, pp. 1–6, April 2016.

[12] H. Bilodeau, S. Babaei, B. Bisewski, J. Burroughs, C. Drover, J. Fenn, B. Fardanesh, B. Tozer, B. Shperling, and P. Zanchette, "Making old new again: Hvdc and facts in the northeastern united states and canada," *IEEE Power and Energy Magazine*, vol. 14, pp. 42–56, March 2016.

[13] H. R. Chamorro, I. Riao, R. Gerndt, I. Zelinka, F. Gonzalez-Longatt, and V. K. Sood, "Synthetic inertia control based on fuzzy adaptive differential evolution," *International Journal of Electrical Power & Energy Systems*, vol. 105, pp. 803 – 813, 2019.

[14] R. Preece, J. V. Milanovic, A. M. Almutairi, and O. Marjanovic, "Probabilistic evaluation of damping controller in networks with multiple vsc-hvdc lines," *IEEE Transactions on Power Systems*, vol. 28, pp. 367–376, Feb 2013.

[15] L. G. Cordero Bautista and P. Bueno de Araujo, "Analysis of the influence of ipfc-pod and pss controllers coordinated tuning by an adaptive genetic algorithm with hyper-mutation," in *2018 Workshop on Communication Networks and Power Systems (WCNPS)*, pp. 1–5, Nov 2018.

[16] L. F. B. Martins, P. B. de Araujo, E. de Vargas Fortes, and L. H. Macedo, "Design of the pi–upfc–pod and pss damping controllers using an artificial bee colony algorithm," *Journal of Control, Automation and Electrical Systems*, vol. 28, pp. 762–773, Dec 2017.

[17] H. R. Chamorro, A. C. Sanchez, A. Pantoja, I. Zelinka, F. Gonzalez-Longatt, and V. K. Sood, "A network control system for hydro plants to counteract the non-synchronous generation integration," *International Journal of Electrical Power & Energy Systems*, vol. 105, pp. 404 – 419, 2019.

[18] E. de Vargas Fortes, P. B. de Araujo, L. H. Macedo, B. R. Gamino, and L. F. B. Martins, "Analysis of the influence of pss and ipfc-pod controllers in small-signal stability using a simulated annealing algorithm," in *2016 12th IEEE International Conference on Industry Applications (INDUSCON)*, pp. 1–8, Nov 2016.

[19] S. L. Ho, , and H. C. W. and, "A simulated annealing algorithm for multiobjective optimizations of electromagnetic devices," *IEEE Transactions on Magnetics*, vol. 39, pp. 1285–1288, May 2003.